Iranian Journal of Chemical Engineering, 17(3), 24-40, (2020) pISSN: 1735-5397
DOI: 10.22034/ijche.2021.259616.1359 eISSN: 2008-2355

Demulsification of Water-in-Oil Emulsions by Means of Dielectrophoresis

M. Mozafari, A. Ganjizade, S. N. Ashrafizadeh [*]

Research Lab for Advanced Separation Processes, Department of Chemical Engineering, Iran University of Science and Technology, Narmak, P. O. Box: 16846-13114, Tehran, Iran

ARTICLE INFO

Article history:
Received: 2020-11-28
Accepted: 2021-01-31

Keywords:
Dielectrophoresis,
Water-in-Oil Emulsion,
Electric Field,
Response Surface Methodology

ABSTRACT

In this work, the demulsification of water-in-crude oil emulsions by dielectrophoresis via applying a non-uniform electric field in a lab-scale cylindrical cell was studied. The stability of emulsions was assessed through monitoring the size distribution of water droplets at 0, 3, 6, and 24 hours after the preparation of emulsion. The effect of operating parameters including the temperature, demulsifier concentration, water salinity, and time on the demulsification of water was investigated. Sodium dodecyl sulfate and sodium chloride were used as demulsifier and salt respectively. The experiments were designed by the response surface methodology (RSM) based on the central composite design (CCD). The operating parameters including the voltage, temperature, demulsifier concentration, salinity of water, and separation time were optimized. The contours and 3-D response surfaces of the water separation were acquired. A quadratic polynomial model, which was statistically highly significant (R^2=0.9950, n=32), was provided by the RSM to predict the amount of the separated water. Comparison among the experimental and RSM-optimized values indicates a good agreement. The optimum amount of the water separation was obtained at the voltage of 15 kV, temperature of 60 °C, demulsifier concentration of 123 ppm, salinity of water of 12260 ppm, and separation time of 12.4 minutes. Under such conditions, the separation of water reached 98 %. The results obviously show that the electric field can be used as an appropriate means for the breakage of W/O emulsions.

1. Introduction

It is well known that the crude water brings several difficulties in petroleum refining industries. Due to the turbulence of the fluid flow during the transportation and processing of crude oil, a part of this water becomes emulsified within the crude oil as small droplets, and water-in-oil (W/O) emulsions are produced [1-3]. The reason behind the droplet formation is the shear force that is applied to crude oil by the transportation energy. These forces increase interfacial area

[*]Corresponding author: Ashrafi@iust.ac.ir (S. N. Ashrafizadeh)

and therefore, lead to the formation of water droplets in the oil phase. Crude oil is a mixture of hydrocarbons comprising asphaltenes, resins, and sand particles. Some of the components such as asphaltenes stabilize the presence of droplets and make the W/O emulsions as a challenge in the petroleum industry [4-6]. Some of the problems being encountered due to this emulsion formation are the corrosion of the pipelines and pumps, a reduction in the catalyst activity during the refining process, and an increase in the operating costs due to the transportation of unusable water, which justify the emulsion breaking [7, 8]. Accordingly, the first stage of the crude oil treatment in the petroleum refineries is the separation of the emulsified water from crude oil [9].

Several emulsion breaking methods including the chemical demulsification [10, 11], filtration [12], application of electric fields [7, 13-15] and heating [16] or a combination of the mentioned methods have been used so far. Electric coagulation methods are appropriate means to improve the yield of the water separation from oil [17]. These methods utilize an electric field to enhance the collision between droplets, droplet size growth, and separation due to sedimentation. As such, these methods are used in electrostatic desalters and dehydrators in the petroleum industry [17-19]. A number of mechanisms including dielectrophoresis, the chain formation of droplets, electrophoresis, the formation of intermolecular bonds, the random collision, the dipole coalescence, and electrofining have been proposed so far [20, 21]. A 3-stage process including (1) droplets approaching one another, (2) the film thinning, and (3) the rupture of film and the coalescence of droplets, has been found responsible for the emulsion breaking.

DEP is defined as the motion of particles (or droplets) due to polarization by a non-uniform electric field [20]. By the polarization of particles or droplets, two equal dipole moments with opposite charges will be induced on two sides of the droplet. In addition to the dispersed phase, the continuous phase would also become polarized. Different polarizability of matters in a mixture can cause a relative motion between them [21]. Droplets with a permittivity greater than that of the continuous phase, e.g. water drops in oil, move towards the place with the most intense electric field (i.e. positive dielectrophoresis) [17, 22]. However, for droplets with a permittivity less than that of the continuous phase, there would be a repulsion force between the droplets and the intense part of the electric field. This force is the reason behind the droplets movement towards the location with the weakest electric field (i.e. negative dielectrophoresis) [23, 24]. One of the advantages of dielectrophoresis (DEP) over processes utilizing uniform electric fields (like electrophoresis) is that the electrodes are not in contact with each other and the unwanted phenomena like electrical short-circuiting doesn't take place due to the formation of water droplet chains [25].

DEP force for a dispersed globular particle in a continuous medium with a relative permittivity of ε_m and an electric field with the intensity of E can be calculated through the following equation:

$$F_{DEP} = 4\pi a^3 \varepsilon_0 \varepsilon_m \mathrm{Re}[K(\varepsilon_p^*.\varepsilon_m^*)](E.\nabla)E \qquad (1)$$

in which "a" is the particle radius, ε_0 is the vacuum permittivity with the value of

8.854×10^{-12} F/m, $\mathrm{Re}[K(\varepsilon_P^*.\varepsilon_m^*)]$ is the real part of the Clausius-Mossoti factor, and E is the intensity of the electric field. The Clausius-Mossoti factor is defined as:

$$K = \frac{\varepsilon_P^* - \varepsilon_m^*}{\varepsilon_P^* + 2\varepsilon_m^*} \quad (2)$$

where ε_P^* and ε_m^* are the complex permittivity of the particles and medium respectively. The complex permittivity can be expressed as:

$$\varepsilon^* = \varepsilon - \frac{j\sigma}{\omega} \quad (3)$$

in which σ is the conductivity of the dispersed or continuous phase; $j = \sqrt{-1}$ and $\omega = 2\pi f$ [26] (f is the frequency of the electric field.)

From the thermodynamics point of view, emulsions will be stabilized by a layer of emulsifiers around the dispersed droplets throughout the emulsion. Asphaltenes and resins are natural emulsifiers in crude oil which stabilize the W/O emulsions through the formation of a rigid viscose film on the interface of water and oil [27].

In this study, the demulsification of the watery crude oil was conducted by applying a non-uniform electric field, i.e. a dielectrophoresis system. One of the Iranian crude oils (Asmari crude oil) was used as the continuous phase. Studying the effect of different parameters on the destabilization of the W/O emulsions was the main objective of this work. The effect of sodium dodecyl sulfate (as a demulsifier), temperature, the water salinity and time, as well as the electric field on the demulsification process was studied. By understanding such effects, one can design a more efficient electrostatic separation system, and better analyze the phenomena taking place in the demulsification of W/O systems.

2. Materials and methods

2.1. Materials

All chemicals were utilized as received and without any further treatment. The specifications of the crude oil which was obtained from one of the Iranian oilfields (Ahwaz Asmari) have been presented in Table 1. The sodium dodecyl sulfate (SDS) surfactant was provided by Sigma-Aldrich Co. (USA) and used as the demulsifier reagent. Deionized water with the pH of 6.8 was used as the dispersed phase. NaCl (Sigma-Aldrich Co. (USA)) was used as the salt.

Table 1
Crude oil specifications.

Specification		Value	Test method
Specific gravity @ 15.56/15.56 °C		0.8621	ASTM D-4052
API		32.63	ASTM D-4052
Base sediment & water (vol %)		<0.05	ASTM D-96
Water content (vol %)		<0.05	ASTM D-95
Salt content (P.T.B)		12.0	ASTM D-3230
Kinematic viscosity (c.St.)	**@ 10 °C**	21.67	ASTM D-445
	@ 20 °C	12.61	ASTM D-4052
	@ 30 °C	6.73	ASTM D-4052
Asphaltenes (wt %)		0.70	IP-143
Wax content (wt %)		5.63	BP-237

2.2. Experimental methods

Emulsions were prepared by mixing certain amounts of SDS and NaCl in 300 mL of distilled water and 2700 mL of crude oil. An Ultra-Turrax T 25 digital homogenizer and an S18N-19G dispersing blade supplied by IKA (Germany) were used for the emulsification of the crude oil. A mixing speed of 9000 rpm and a mixing time of 10 min were exerted for emulsification purposes. The prepared emulsions were immediately transferred into the separation cell to rest.

The size distribution of droplets was measured through image capturing by a Huvitz HRM300BD-RT microscope (South Korea) at either of 0, 3, 6, and 24 hours after the emulsion formation. Samples were taken from middle depth of the bulk emulsion and were dripped on a glass slide, and images were taken from several positions of each slide. Afterwards, the images were analyzed by the Image J processing software to measure the droplet size distribution. To make the water droplets distinguishable from their surroundings and from each other, the images were first converted into 8-bit images and then their quality was improved by some features of the software, i.e. smoothing and brightening. Afterwards, the number of water droplets was identified by the process toolbox of the Image J software and the surface area of each droplet was calculated subsequently. Having the surface area of each droplet, the diameters of droplets were determined. Eventually, the histogram of the size distribution of droplets was generated by the Minitab statistics software. Figure 1 illustrates the employed analysis procedure for the emulsion images. Through comparing Figures 1B and 1D it becomes evident that almost all droplets were distinguished and detected.

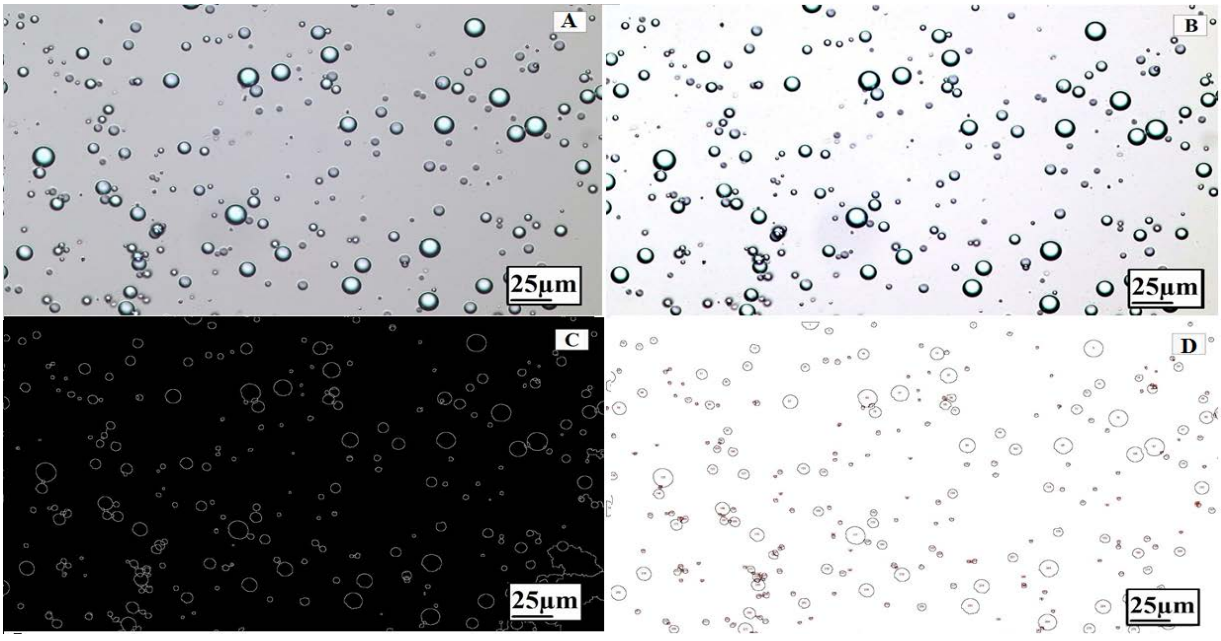

Figure 1. Procedure of the emulsion microscopic image analysis, A) Original image, B) Processed image by smooth and brighten filters, C) Processed image by process toolbox (droplet detection), D) Count and analysis of droplets.

The separation cell, comprising of two coaxial chambers, was made of glass. The main (inner) chamber, which is mainly a vessel for the emulsion, is equipped with two

electrodes: *i)* an electrode bar of the diameter of 5 mm at the centeral axis of the chamber and *ii)* a cylindrical shape electrode attached to the chamber's wall, surrounding the bar electrode and the emulsion. It must be noted that the bar electrode has been surrounded by an insulator. The outer chamber, which is a jacket for the water circulation, has been connected to the water bath for adjusting temperature. The temperature of the water bath was monitored by means of a thermometer, and using a controller, the water temperature was tuned to a set point. It is assumed that the coefficient of the heat transfer between the cooling water and the emulsion is so high that their temperatures can be considered almost equal. The inner container, with the diameter, wall thickness, and height of 16, 0.5 and 19 cm respectively, had a capacity of about 4 liters. At the conical bottom of the inner container, a valve was installed for discharging the separated water. The experimental apparatus including the cell and electrodes as well as the whole set-up have been schematically shown in Figures 2 and 3.

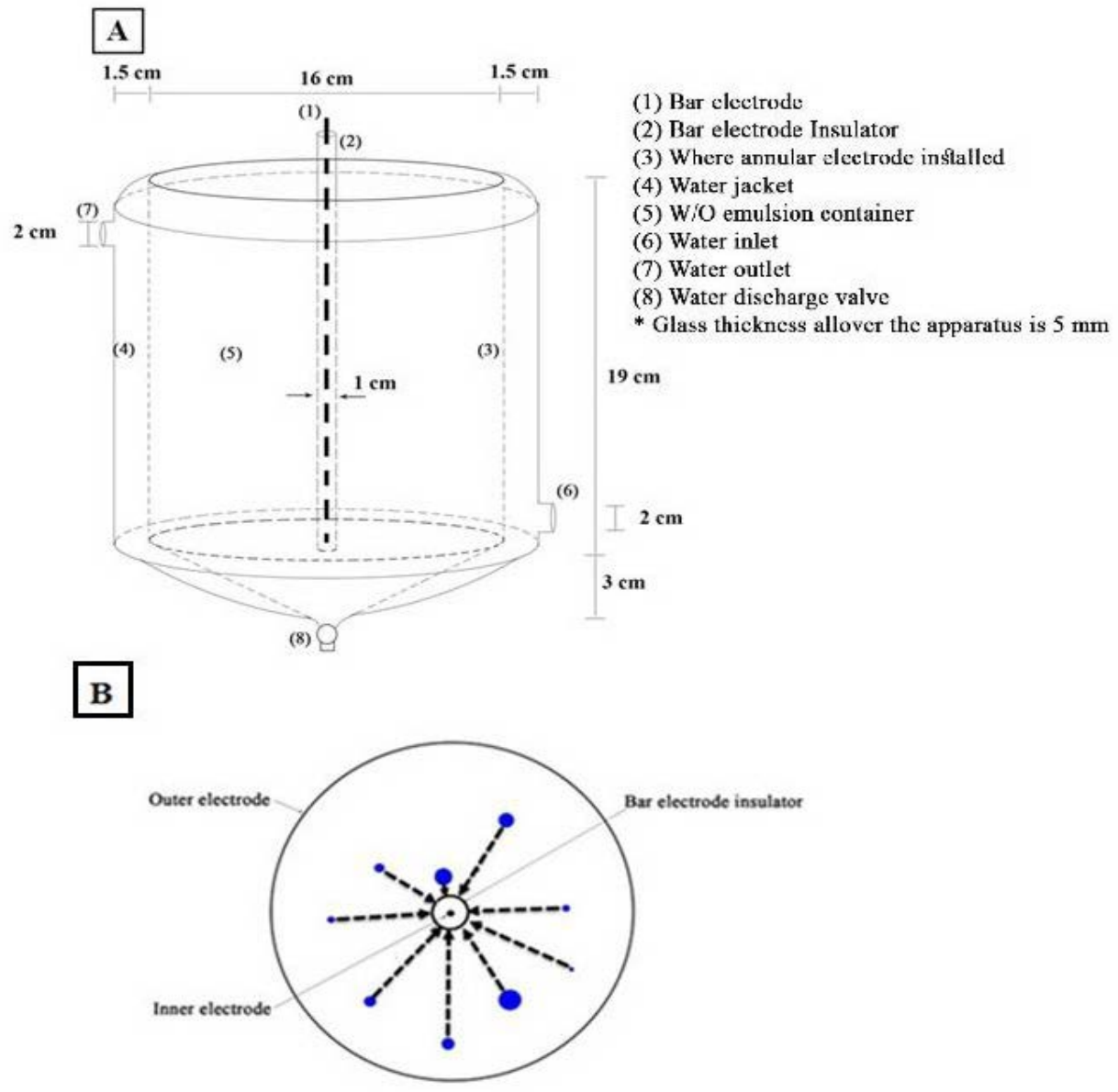

Figure 2. A) Cell and electrodes arrangement, B) schematic of droplet movements.

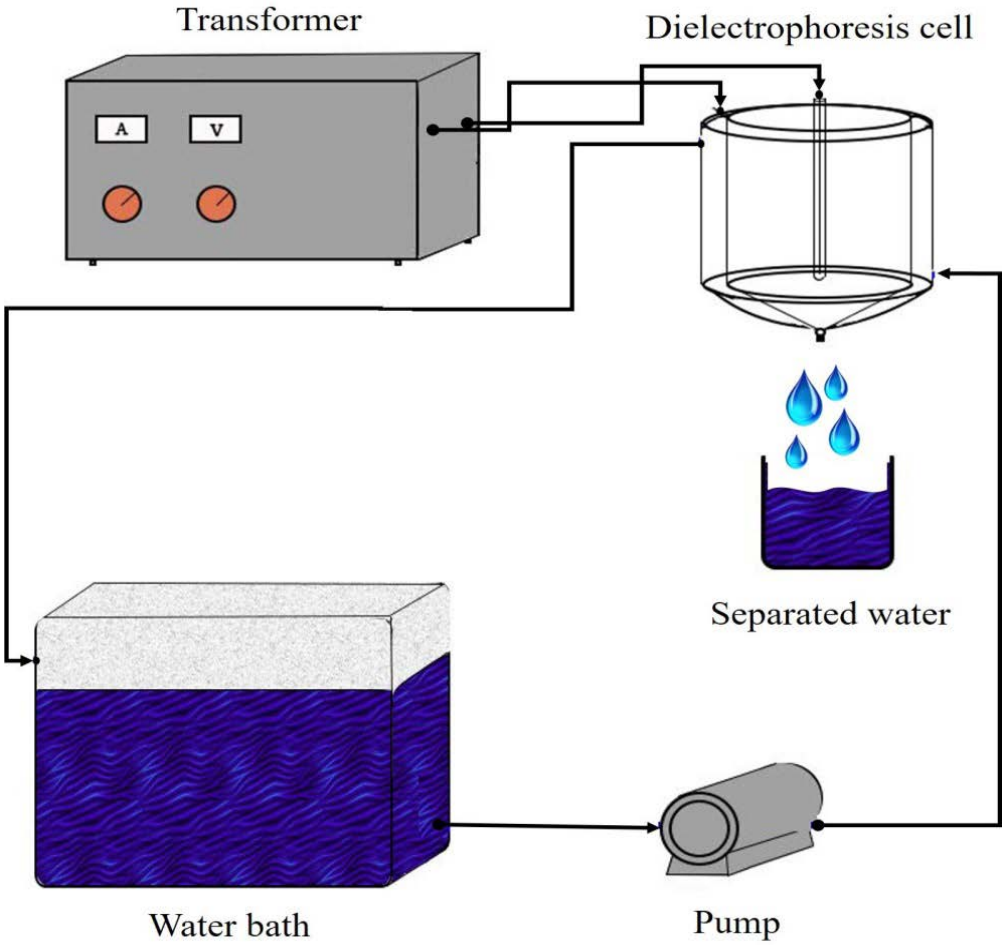

Figure 3. Experimental apparatus.

The two copper electrodes connected to a transformer were used to supply the alternating current (AC). The produced non-uniform electric field with the frequency of 50 Hz was applied to the emulsion. The electric field was directed toward the center of the inner container and the most powerful electric field was held in the center.

The amount of the separated water (% WS) was determined through Eq. (4):

$$\% \text{ WS} = \frac{V_s}{V_t} \times 100 \quad (4)$$

where V_s is the volume of the separated water and V_t represents the total volume of the emulsified water (300 mL).

2.3. Experimental design

Design Expert 10 was used to design the experiments by a 1/2 fraction factorial CCD of the RSM. A number of 32 tests, which consist of 6 center points ($\alpha = 2$), were conducted to study the effects of parameters and important variables on the separation of water from crude oil. The independent variables in this work were voltage (A), temperature (B), the demulsifier concentration (C), the water salinity (D) and time (E), while the amount of the separated water was chosen as the response. The ranges and levels of each variable are given in Table 2. Design Expert 10 was used to perform a regression analysis of the data and to estimate the response function. The results of experimental data are presented in Table 3.

Table 2
Ranges and levels of all independent variables.

Variables	Levels				
	-α	-1	0	1	α
Voltage (kV), A	0.00	3.75	7.50	11.25	15.00
Temperature (°C), B	30.0	37.5	45.0	52.5	60.0
Demulsifier concentration (ppm), C	0	50	100	150	200
Water salinity (ppm), D	0	6250	12500	18750	25000
Separation time (min), E	2.00	5.25	8.50	11.75	15.00

Table 3
Central composite design of the experiments of the water separation from the W/O emulsion.

Run Order	Voltage (kV)	Temperature (°C)	Demulsifier Conc. (ppm)	Salinity (ppm)	Time (min)	Separated water (mL)	Response: water separation (%)
	A	B	C	D	E		R
1	7.50	60.0	100	12500	8.50	234	78.0
2	11.25	52.5	150	18750	11.75	255	85.0
3	3.75	52.5	150	6250	11.75	195	65.0
4	7.50	45.0	100	12500	2.00	133	44.3
5	7.50	45.0	100	12500	8.50	206	68.7
6	7.50	45.0	100	25000	8.50	194	64.7
7	3.75	37.5	50	18750	5.25	89	29.7
8	11.25	52.5	50	6250	11.75	219	73.0
9	7.50	45.0	0	12500	8.50	121	40.3
10	11.25	37.5	150	6250	11.75	222	74.0
11	7.50	30.0	100	12500	8.50	157	52.3
12	3.75	37.5	150	18750	11.75	156	52.0
13	7.50	45.0	100	0	8.50	150	50.0
14	7.50	45.0	100	12500	8.50	209	69.7
15	7.50	45.0	100	12500	8.50	211	70.3
16	3.75	52.5	150	18750	5.25	129	43.0
17	11.25	52.5	150	6250	5.25	231	77.0
18	7.50	45.0	100	12500	8.50	198	66.0
19	7.50	45.0	200	12500	8.50	186	62.0
20	11.25	37.5	50	18750	11.75	207	69.0
21	11.25	52.5	50	18750	5.25	219	73.0
22	3.75	52.5	50	18750	11.75	189	63.0
23	15.00	45.0	100	12500	8.50	250	83.3
24	7.50	45.0	100	12500	8.50	199	66.3
25	3.75	37.5	150	6250	5.25	99	33.0
26	11.25	37.5	50	6250	5.25	141	47.0
27	3.75	52.5	50	6250	5.25	102	34.0
28	7.50	45.0	100	12500	8.50	204	68.0
29	11.25	37.5	150	18750	5.25	180	60.0
30	0.00	45.0	100	12500	8.50	93	31.0
31	3.75	37.5	50	6250	11.75	96	32.0
32	7.50	45.0	100	12500	15.00	227	75.7

A quadratic model was generated to describe the relationship between the response and operational parameters as defined by Eq. (5):

$$y = \alpha_0 + \sum_{i=1}^{3} \alpha_i x_i + \sum_{i=1}^{3} \alpha_{ii} x_i^2 + \sum_{i=1}^{2} \sum_{i=1}^{3} \alpha_{ij} x_i x_j + \epsilon \quad (5)$$

where y is the predicted response (the estimated separation percentage), x_i, x_j are the independent variables, α_i, α_{ij} are the estimated coefficients from regression for linear and binary interaction effects on the response respectively, and α_{ii}s are coefficients estimated from the regression for quadratic effects. The parameters α_0 and ϵ are the model constant coefficient and model random error. Analysis of variance (ANOVA) was used to analyze the results. A P-value of ≤ 0.05 shows that the term is important. 3D and contour diagrams of the results are presented to determine the effects of variables on the response.

3. Results and discussion

3.1. Emulsion stability

In order to study the stability of water-in-crude oil emulsions, the size distribution of water droplets at 0, 3, 6, and 24 hours after the preparation of emulsion was monitored. It must be mentioned that the samples were taken from the middle depths of the emulsions level. The size distribution of droplets at the mentioned time intervals, obtained from the data of Figure 1, is presented in Figure 4. In this Figure, a 3-parameter Weibull probability distribution function, due to its highest p-value compared to other functions (Table 4), was used to model the droplet size distribution of the emulsions at various time intervals. Figure 4 also shows that as time passes, the number of droplets decreases. This observation is due to the droplets coalescing, formation of larger droplets, settlement over time due to gravity and finally formation of a separate aqueous phase.

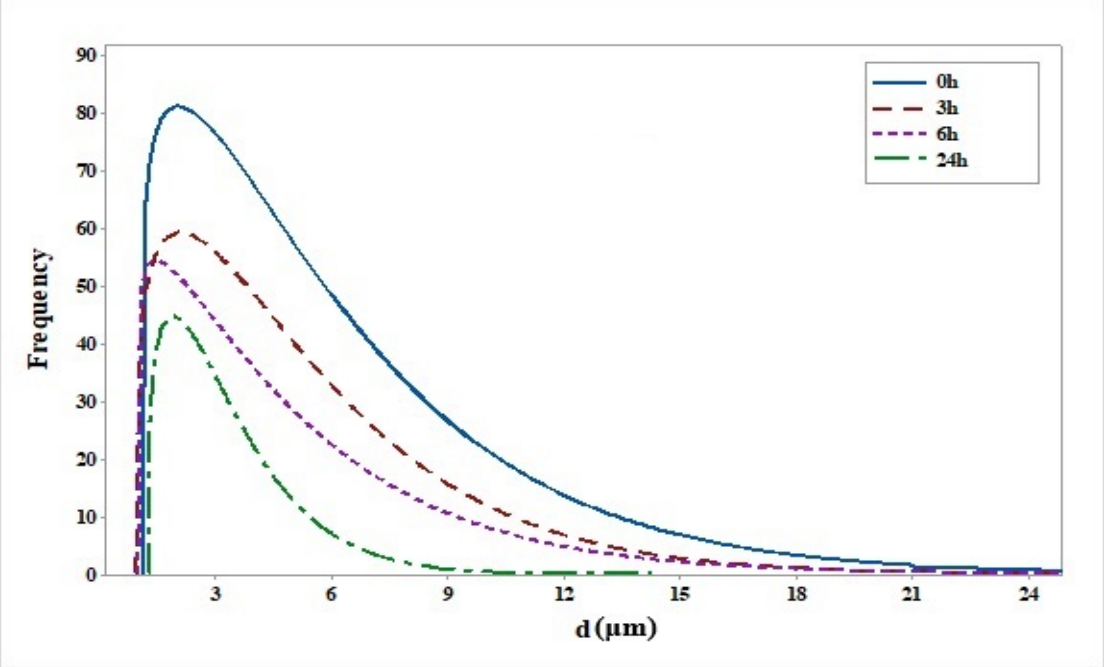

Figure 4. Distribution of water droplets size at 0, 3, 6 and 24 hours after the emulsion formation.

Table 4
P-values of different probability distribution functions.

Distribution	P-value			
	0 hr	**3 hr**	**6 hr**	**24 hr**
Normal	<0.005	<0.005	<0.005	<0.005
Lognormal	<0.005	<0.005	0.007	<0.005
3-Parameter Lognormal	*	*	*	*
Exponential	<0.003	<0.003	<0.003	<0.003
2-Parameter Exponential	<0.010	<0.010	0.029	<0.010
Weibull	<0.010	<0.010	<0.010	<0.010
3-Parameter Weibull	0.081	0.031	0.040	0.041
Smallest Extreme Value	<0.010	<0.010	<0.010	<0.010
Largest Extreme Value	<0.010	<0.010	<0.010	<0.010
Gamma	<0.005	<0.005	<0.005	<0.005
3-Parameter Gamma	*	*	*	*
Logistic	<0.005	<0.005	<0.005	<0.005
Loglogistic	<0.005	<0.005	<0.005	<0.005
3-Parameter Logistic	*	*	*	*

* Symbol shows that p-value cannot be calculated by Minitab .

3.2. Effect of variables on the water separation

In this section, the results gained by means of calculations, performed by Design Expert, are presented.

3.2.1. Effect of voltage

The efficacy of the voltage in the range of 0-15 kV (RMS) on the water separation was studied. The temperature, demulsifier concentration, salinity of water and duration of applying the electric field were 45 °C, 100 ppm, 12500 ppm and 8.5 min respectively. The results which are shown in Figure 5A exhibit that the water separation was increased by the increase in the voltage from 0 to 15 kV. Such an observation can be attributed to the fact that, the more the electric field, the more the bipolarization and the more velocity of the droplets. This leads to faster movement of the droplets towards the strong electric zone, higher collision, formation of larger droplets and more intensive settlement. The direction of the droplets movement according to the above mentioned fact is presented in Figure 2B.

3.2.2. Effect of temperature

The amount of the separated water by the increase in the emulsion temperature from 30 to 60 °C at the voltage of 7.5 kV, demulsifier concentration of 100 ppm, water salinity of 12500 ppm and duration of 8.5 min was studied. The results which are exhibited in Figure 5B reveal that the increase in temperature leads to an increase in the water separation. The first reason for this observation is a reduction in the viscosity of the continuous phase which enhances the droplets movement and facilitates their

collisions. The second reason is that the increase in temperature leads to weakening the layer of asphaltenes around the droplets which improves demulsification. Moreover, the two other side effects of raising temperature on the real industrial scale should be also considered. First, the volatile components of crude oil would vaporize at high temperatures and reduce the crude price. Second, the air bubbles would form under such conditions and stick to droplets surfaces, resulting in the absorption of surfactants. It should be reminded that these droplets would not separate by sedimentation and remain in crude oil. As such, the application of high temperatures is not recommended in this work.

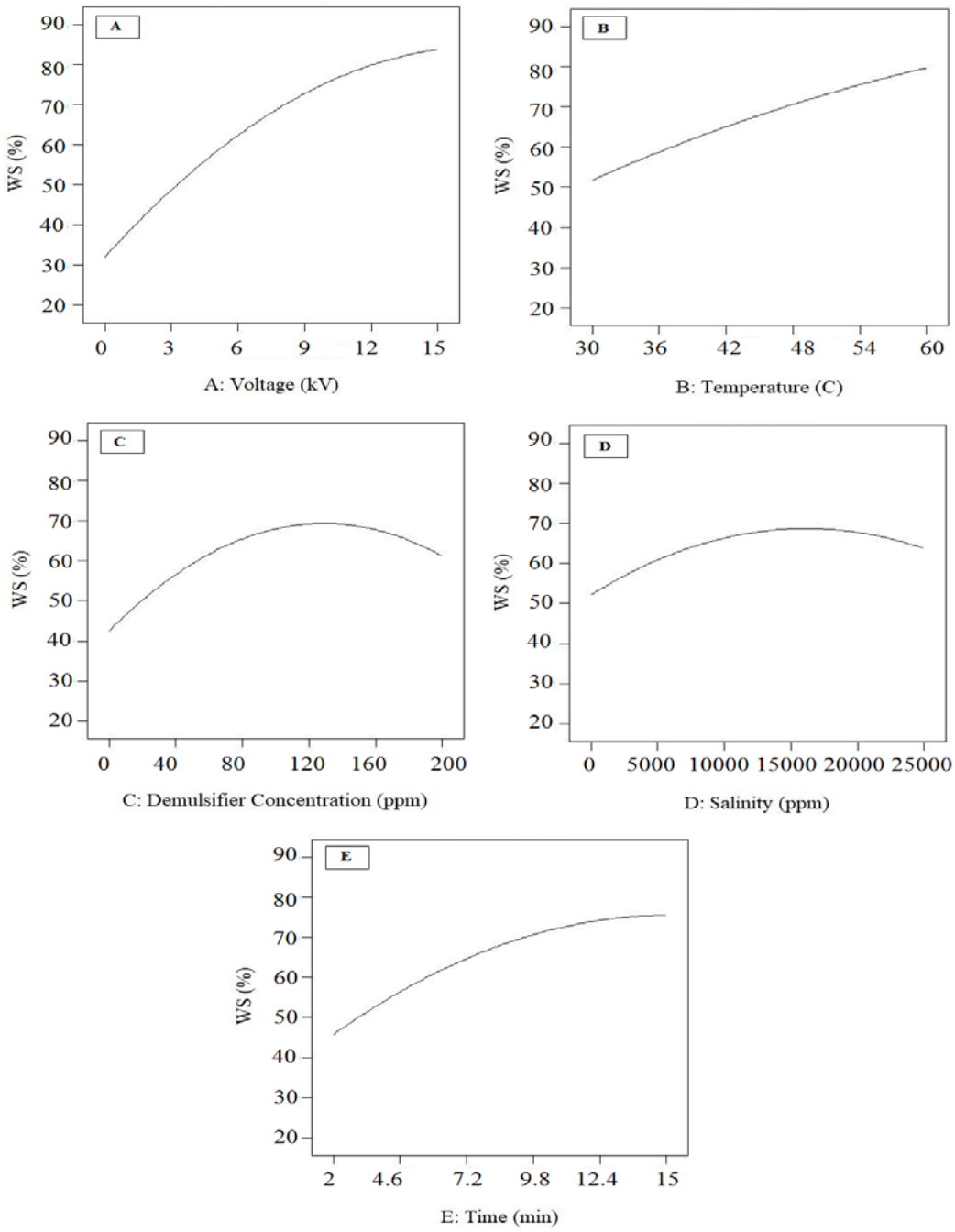

Figure 5. Effects of independent variables on the water separation, while other variables are at zero levels: A) Voltage, B) Temperature, C) Demulsifier Concentration, D) Salinity, E) Time.

3.2.3. Effect of demulsifier concentration

The effect of the demulsifier concentration on the water separation is presented in Figure 5C. The voltage, temperature, salinity of water and time were fixed at 7.5 kV, 45 °C, 12500 ppm and 8.5 min respectively. Figure 5C indicates that for demulsifier concentrations of less than about 125 ppm, the more the demulsifier concentration, the more the separation. However, demulsifier concentrations behind that limit did not improve the water separation. It is notable that demulsifiers intensify the film drainage before it tears apart. This is because of the coverage of all interfaces with demulsifier molecules [28]. In W/O emulsions, demulsifiers move across the free spaces among the aggregates of asphaltene and become adsorbed at the interface [28]. This phenomenon leads to the aggregates of asphaltenes and droplet surface parting and facilitates the droplets coagulation. Besides, the addition of further demulsifier causes the formation of a layer of demulsifier around the droplets and reduces the water separation. This phenomenon is called the "overdose effect" [29-31] in the oil industry.

3.2.4. Effect of salinity

The effect of the salinity of water on the separation of water is shown in Figure 5D. The voltage, temperature, demulsifier concentration and time were 7.5 kV, 45 °C, 100 ppm, and 8.5 min respectively. As it is apparent, the increase in the salinity of water from 6250 ppm to about 17000 ppm improves the water separation. It can be said that the more the water salinity, the more the interfacial tension between water droplets and the oil, and the less the interfacial area-per-volume. Consequently, the higher water salinity triggers, to some extent, the formation of larger droplets and the faster coalescence of water. In addition, the raise in the salinity of water would boost the ionic strength as well as the electrostatic attraction among droplets. The addition of further amounts of salt leads to an increase in the electrostatic repulsion and thus a slight reduction in the water separation.

3.2.5. Effect of the process duration

The effect of the process duration on the water separation is shown in Figure 5E. The voltage, temperature, demulsifier concentration and salinity of water were 7.5 kV, 45 °C, 100 ppm and 12500 ppm respectively. According to Figure 5E, with the passage of time, more water is separated. The reason behind this observation is that the emulsion is more affected by the electric field, demulsifier and heat. Moreover, water droplets have more time to settle down and become separated.

3.3. Statistics and experimental design results

3.3.1. Regression model and analysis of variance

A full quadratic polynomial model was developed to predict the influence of operational variables on the separation yield (Eq. 6). It must be mentioned that this model is specific to our system's configuration.

$$\begin{aligned}\%\,\mathrm{WS} = {} & -138.15 + 7.69\mathrm{A} + 2.15\mathrm{B} + 0.638\mathrm{C} + 3.67\times10^{-3}\mathrm{D} + 5.36\mathrm{E} - 7.40\times10^{-4}\mathrm{AB} - 7.40\\ & \times10^{-4}\mathrm{AC} - 2.04\times10^{-5}\mathrm{AD} - 0.14\mathrm{AE} - 2.38\times10^{-3}\mathrm{BC} - 1.28\times10^{-5}\mathrm{BD} + 4.27\\ & \times10^{-3}\mathrm{BE} - 1.15\times10^{-5}\mathrm{CD} + 3.71\times10^{-3}\mathrm{CE} + 3.17\times10^{-5}\mathrm{DE} - 0.18\mathrm{A}^2 - 9.49\\ & \times10^{-3}\mathrm{B}^2 - 1.61\times10^{-3}\mathrm{C}^2 - 6.38\times10^{-8}\mathrm{D}^2 - 0.17\mathrm{E}^2\end{aligned} \quad (6)$$

The predicted response of the water separation versus the actual response is shown in Figure 6. Regarding the data points which are close to the 45° line, there is a good agreement between actual and predicted responses. According to Figure 6, the model accuracy is high (R^2=0.99, n=32). Table 5 shows the analysis of the variance result (ANOVA). The p-values of less than 0.05 reveal significant terms of the equation and other terms are considered insignificant. In this case, A, B, C, D, E, AE, BC, CD, A2, C2, D2, and E2 are significant terms of the model. The F-value of 109.78 and p-value of less than 0.0001 denote the model being significant. Further, the adjusted R^2 and the predicted R^2 of the model are 0.98 and 0.86 respectively. The difference between the adjusted R^2 and the predicted R^2 is less than 0.2, which demonstrates their reasonable agreement. The adequate precision value provided in Table 5 is 35.51 which indicates the model is appropriate for the statistical design and data analysis.

3.3.2. Optimization of process parameters by the RSM

The optimum level of each process parameter was determined to specify the maximum percentage of the water separation (Response). Moreover, some of 2-D and 3-D graphs of response surface curves were drawn by using a full quadratic polynomial regression model equation. These graphs have been plotted by changing the quantities of two variables and keeping other variables fixed at their zero levels. Figures 7A and 7B depict the interaction between the voltage and the process duration. The contour plots disclose the optimal voltage being around 12-15 kV and the optimal time being around 9-15 min. From Figures 7C and 7D, it is obvious that the increase in the demulsifier concentration from 110 to 160 ppm turns the water separation up to about 69 % and then shows a drop. These Figures also exhibit the separation of water being improved by raising the water salinity up to about 11000-17000 ppm and then demonstrates a slight decrease. Figures 7E and 7F present the effects of the temperature and demulsifier concentration on the water separation. It is apparent that the emulsion breaking is improved by raising the temperature. The maximum values of the emulsion breaking were obtained in the range of 57-60 °C.

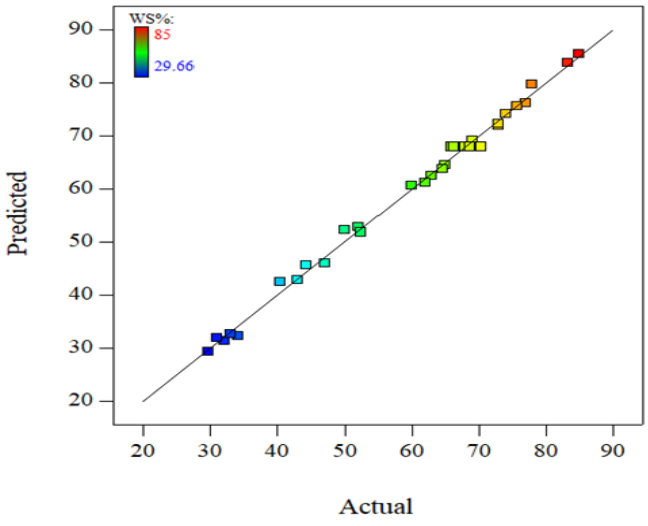

Figure 6. The predicted responses of the water separation versus the actual response.

Table 5
Analysis of the variance of quadratic model for the water separation from crude oil emulsions.

Source	Sum of squares	df	Mean square	F-value	P-value	Remark
Model	8327.42	20	416.37	109.78	< 0.0001	Significant
A	4030.04	1	4030.04	1062.55	< 0.0001	
B	1171.34	1	1171.34	308.83	< 0.0001	
C	519.56	1	519.56	136.99	< 0.0001	
D	198.38	1	198.38	52.30	< 0.0001	
E	1335.04	1	1335.04	351.99	< 0.0001	
AB	6.943×10^{-3}	1	6.943×10^{-3}	1.83×10^{-3}	0.9666	
AC	6.943×10^{-3}	1	6.943×10^{-3}	1.83×10^{-3}	0.9666	
AD	3.67	1	3.67	0.97	0.3462	
AE	50.17	1	50.17	13.23	0.0039	
BC	12.84	1	12.84	3.39	0.0929	
BD	5.84	1	5.84	1.54	0.2405	
BE	0.17	1	0.17	0.046	0.8345	
CD	207.84	1	207.84	54.80	< 0.0001	
CE	5.84	1	5.84	1.54	0.2405	
DE	6.67	1	6.67	1.76	0.2116	
A^2	188.37	1	188.37	49.66	< 0.0001	
B^2	8.37	1	8.37	2.21	0.1655	
C^2	477.37	1	477.37	125.86	< 0.0001	
D^2	182.22	1	182.22	48.04	< 0.0001	
E^2	97.78	1	97.78	25.78	0.0004	
Residual	41.72	11	3.79			
Lack-of-fit	26.44	6	4.41	1.44	0.3523	Insignificant
Pure error	15.28	5	3.06			
Cor total	8369.14	31				
Std. Dev.	1.95		R-squared	0.99		
Mean	59.39		Adj R-squared	0.98		
C.V. %	3.28		Pred R-squared	0.91		
PRESS	706.47		Adeq precision	35.51		

In summary, the optimal values of process variables were in the ranges of; the voltage: 12-15 kV, the temperature: 57-60 °C, the demulsifier concentration: 110-160 ppm, the water salinity: 11000-17000 ppm and the process duration: 9-15 min.

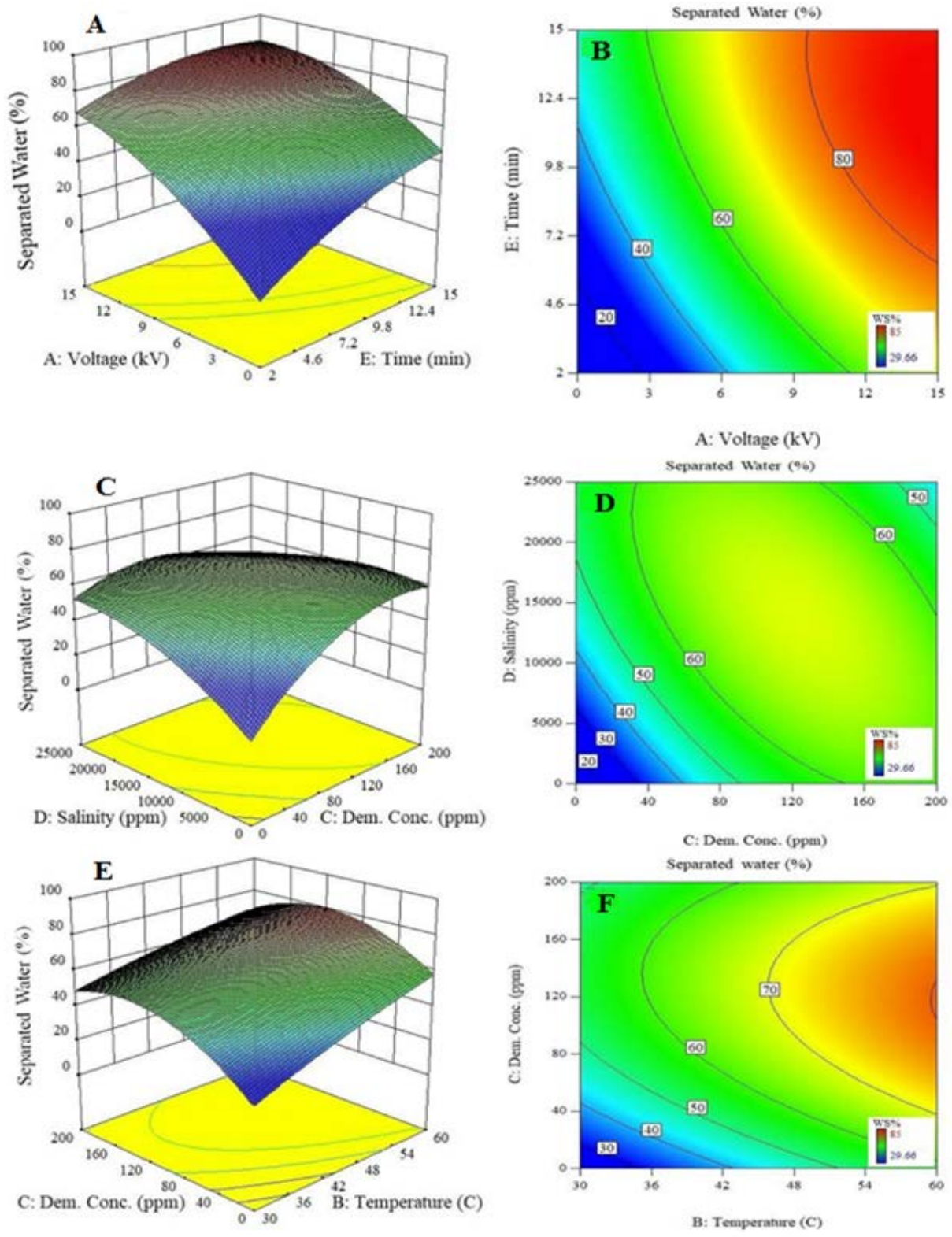

Figure 7. A) 3-D graph and B) response surface contours for the water separation; the interaction between voltage and time, C) 3-D graph and D) response surface contours for the water separation; the interaction between the demulsifier concentration and the water salinity, E) 3-D graph and F) response surface contours for the water separation; the interaction between temperature and the demulsifier concentration. A and B) the water salinity: 12500 ppm; temperature: 45 °C; the demulsifier concentration: 100 ppm. C and D) voltage: 7.5 kV; the separation time: 8.5 min; temperature: 45 °C. E and F) voltage: 7.5 kV; the water salinity: 12500 ppm; the separation time: 8.5 min.

Further, the optimization of process variables was conducted by the design of experiments. The optimized values of the voltage, temperature, demulsifier concentration, water salinity and process duration were found: 15 kV, 60 °C, 123 ppm, 12260 ppm and 12.4 min respectively. Under the mentioned conditions, the water separation was predicted to be 98 %. Such a high prediction may be attributed to other probable phenomena taking place in process which are unintentionally overlooked. This shortcoming must be fixed in the future studies. The observed notable agreement between the optimized amounts of parameters, figured out experimentally and those estimated mathematically, proves that the model is able to work out the water separation from the water-in-crude oil emulsions.

4. Conclusions

The aim of this work was to investigate the behavior of the dielectrophoresis system in the separation of water from W/O emulsions. For that purpose, an emulsion was prepared by homogenizing water in one of the Iranian crude oils. The effects of various process variables including the voltage, temperature, demulsifier concentration, salinity of water and process duration on the water separation were investigated. Moreover, the process variables were optimized by response surface methods according to the central composite design and the results of the optimization were compared with the experimental values. The comparison between the RSM optimized parameters and experimental results, indicated that all values were in good agreement with one another. The analysis of variance (ANOVA) was used to show the significance of and interactions between parameters in the emulsion breaking process. A significant quadratic polynomial equation, which could clarify the behavior of the W/O emulsion breaking, was provided by ANOVA. The model optimum conditions, which were calculated by the RSM, were obtained as: the voltage of 15 kV, temperature of 60 °C, demulsifier concentration of 123 ppm, water salinity of 12260 ppm and process duration of 12.4 min. It must be noted that the suggested model suffers from some limitations including neglecting Joule heating, neglecting the functionality of the system's temperature form the parameters influencing Joule heating, neglecting the heterogeneity of the water content inside the emulsion, etc. This must be addressed in the future works. The results of this study reveal that the water separation from Asmari crude oil emulsions under the optimum conditions has a remarkable potential for the complete separation of water, i.e. 98 %.

Acknowledgement

The research council at Iran University of Science and Technology (IUST) is highly appreciated for its financial support during the course of this research.

Declaration of interests

The authors declare that they have no known competing financial interest or personal relationship that could have appeared to influence the work reported in this paper.

References

[1] Hajivand, P. and Vaziri, A., "Optimization of demulsifier formulation for separation of water from crude oil emulsion", *Brazilian J. Chem. Eng.*, **32**, 107 (2015).

[2] Kokal, S., Crude oil emulsions, Petroleum engineering handbook, (2006).

[3] Smith, H. V. and Arnold, K., Crude oil emulsions (1987 PEH Chapter 19), Petroleum engineering handbook, (1987).

[4] Rodionova, G., Kelesoglu, S. and Sjöblom, J., "AC field induced destabilization of water-in-oil emulsions based on North Sea acidic crude oil", *Colloids Surfaces A Physicochem Eng. Asp.*, **448**, 60 (2014).

[5] Kilpatrick, P. and Spiecker, P., Asphaltene emulsions, Marcel Dekker, New York, (2001).

[6] Ashtari, M., Ashra, S. N. and Bayat, M., "Asphaltene removal from crude oil by means of ceramic membranes", *J. Pet. Sci. Eng.*, **82-83**, 44 (2012).

[7] Li, Q., Chen, J., Meng, L., Liang, M., Pan, Z. and Wang, K., "Investigation of water separation from water-in-oil emulsion using high frequency pulsed AC electric field by new equipment", *J. Dispers. Sci. Technol.*, **36**, 918 (2015).

[8] Verruto, V. J., Le, R. K. and Kilpatrick, P. K., "Adsorption and molecular rearrangement of amphoteric species at oil-water interfaces", *J. Phys. Chem. B*, **113**, 13788 (2009).

[9] Mohammadi, M., Shahhosseini, S. and Bayat, M., "Direct numerical simulation of water droplet coalescence in the oil", *Int. J. Heat. Fluid Flow*, **36**, 58 (2012).

[10] Wu, J., Xu, Y., Dabros, T. and Hamza, H., "Effect of demulsifier properties on destabilization of water-in-oil emulsion", *Energy and Fuels*, **17**, 1554 (2003).

[11] Yi, M., Huang, J. and Wang, L., "Research on crude oil demulsification using the combined method of ultrasound and chemical demulsifier", *J. Chem.*, **2017**, (2017).

[12] Venault, A., Jumao-as-Leyba, A. J., Chou, F. C., Bouyer, D., Lin, I. J., Wei, T. C. and Chang, Y., "Design of near-superhydrophobic/superoleophilic PVDF and PP membranes for the gravity-driven breaking of water-in-oil emulsions", *J. Taiwan Inst. Chem. Eng.*, **0**, 1 (2016).

[13] Zhang, L., He, L., Ghadiri, M. and Hassanpour, A., "Effect of surfactants on the deformation and break-up of an aqueous drop in oils under high electric field strengths", *J. Pet. Sci. Eng.*, **125**, 38 (2015).

[14] Muto, A., Matsumoto, T. and Tokumoto, H., "Continuous flow demulsification of a water-in-toluene emulsion by an alternating electric field", *Sep. Purif. Technol.*, **156**, 175 (2015).

[15] Yang, D., Xu, M., He, L., Luo, X., Lü, Y., Yan, H. and Tian, C., "The influence and optimisation of electrical parameters for enhanced coalescence under pulsed DC electric field in a cylindrical electrostatic coalescer", *Chem. Eng. Sci.*, **138**, 71 (2015).

[16] Kar, T. and Hascakir, B., "The role of resins, asphaltenes, and water in water-oil emulsion breaking with microwave heating", *Energy and Fuels*, **29**, 3684 (2015).

[17] Eow, J. S., Ghadiri, M., Sharif, A. O. and Williams, T. J., "Electrostatic enhancement of coalescence of water droplets in oil: A review of the current understanding", *Chem. Eng. J.*, **84**, 173 (2001).

[18] Eow, J. S. and Ghadiri, M., "Electrostatic enhancement of coalescence of water droplets in oil: A review of the technology", *Chem. Eng. J.*, **85**, 357 (2002).

[19] Sun, D., Duan, X., Li, W. and Zhou, D., "Demulsification of water-in-oil emulsion by using porous glass

membrane", *J. Memb. Sci.*, **146**, 65 (1998).

[20] Pethig, R., "Dielectrophoresis: Status of the theory, technology, and applications", *Biomicrofluidics*, **4**, 022811 (2010).

[21] Monfared, M. A., Kasiri, N. and Mohammadi, T., "A CFD model for prediction of critical electric potential preventing membrane fouling in oily waste water treatment", *J. Memb. Sci.*, **539**, 320 (2017).

[22] Pohl, H. A., The motion and precipitation of suspensoids in divergent electric fields", *J. Appl. Phys*., **22**, 869 (1951).

[23] Molla, S. H. and Bhattacharjee, S., "Prevention of colloidal membrane fouling employing dielectrophoretic forces on a parallel electrode array", *J. Memb. Sci.*, **255**, 187 (2005).

[24] Du, F., Hawari, A. and Baune, M., "Dielectrophoretically intensified cross-flow membrane filtration", *J. Memb. Sci.*, **336**, 71 (2009).

[25] Alinezhad, K., Hosseini, M., Movagarnejad, K. and Salehi, M., "Experimental and modeling approach to study separation of water in crude oil emulsion under non-uniform electrical field", *Korean J. Chem. Eng.*, **27**, 198 (2010).

[26] Du, F., Ciaciuch, P., Bohlen, S., Wang, Y., Baune, M. and Thöming, J., "Intensification of cross- flow membrane filtration using dielectrophoresis with a novel electrode configuration", *J. Memb. Sci.*, **448**, 256 (2013).

[27] Xia, L., Lu, S. and Cao, G., "Stability and demulsification of emulsions stabilized by asphaltenes or resins", *J. Colloid Interface Sci.*, **271**, 504 (2004).

[28] Daniel-David, D., Le Follotec, A., Pezron, I., Dalmazzone, C., Noik, C., Barre, L. and Komunjer, L., "Destabilisation of water-in-crude oil emulsions by silicone copolymer demulsifiers", *Oil Gas Sci. Technol.*, **63**, 165 (2008).

[29] Chong, J. Y., Machado, M. B., Bhattacharya, S., Ng, S. and Kresta, S. M., "Reduce overdosing effects in chemical demulsifier applications by increasing mixing energy and decreasing injection concentration", *Energy and Fuels*, **30**, 5183 (2016).

[30] Xu, Y., Wu, J., Dabros, T. and Hamza, H., "Optimizing the polyethylene oxide and polypropylene oxide contents in diethylenetriamine-based surfactants for destabilization of a water-in-oil emulsion", *Energy and Fuels*, **19**, 916 (2005).

[31] Dimitrov, A. N., Yordanov, D. and Petkov, P. S., "Study on the effect of demulsifers on crude oil and petroleum products", *Int. J. Environ. Res.*, **6**, 435 (2012).